Available online at www.sciencedirect.com
SCIENCE DIRECT®
Journal of Nuclear Materials 349 (2006) 119–132
journal of nuclear materials
www.elsevier.com/locate/jnucmat

Displacement cascades in Fe–Cr: A molecular dynamics study

D.A. Terentyev [a,b], L. Malerba [a,*], R. Chakarova [c], K. Nordlund [d], P. Olsson [e], M. Rieth [f], J. Wallenius [c]

[a] SCKCEN, The Belgian Nuclear Research Centre, Boeretang 200, B-2400 Mol, Belgium
[b] Physique des Solides Irradiés et des Nanostructure CP234s, Université Libre de Bruxelles Bd. du Triomphe, B-1050 Brussels, Belgium
[c] Department of Nuclear and Reactor Physics, Royal Institute of Technology, Roslagstullsbacken 21, SE-106 91 Stockholm, Sweden
[d] Accelerator Laboratory, University of Helsinki, P.O. Box 43 (Pietari Kalmin katu 2) FIN-00014, Finland
[e] Department of Neutron Research, Ångstrom Laboratory, Uppsala University, P.O. Box 525, SE-751 20 Uppsala, Sweden
[f] Forschungszentrum Karlsruhe, Institute for Materials Research I, P.O. Box 3640, 76021 Karlsruhe, Germany

Received 6 July 2005; accepted 26 October 2005

Abstract

Displacement cascades up to 50 keV have been simulated in Fe–10%Cr by molecular dynamics (MD), using an embedded-atom method (EAM) interatomic potential which satisfactorily reproduces the interaction between Cr atoms and point-defects in α-Fe. In particular, the potential can reproduce the strong interaction with self interstitial atoms characteristic of Fe–Cr alloys. The results, when compared to the case of pure Fe, show that the presence of Cr does not significantly influence either the ballistic phase of the cascade, or the primary damage state, in terms of number of surviving defects or clustered fraction. However, the fraction of Cr atoms in interstitial position greatly exceeds the alloy concentration, in agreement with some experimental indications, and this feature is expected to influence the long-term evolution of radiation damage in the alloy. The mechanisms leading to the accumulation of Cr in interstitial positions and the expected trapping effect on interstitial clusters are analysed and discussed.

PACS: 31.15.Qg; 61.72.Cc; 61.72.Ji; 61.82.Bg

1. Introduction

High-Cr, reduced-activation ferritic/martensitic (RAFM) steels are receiving special attention as potential structural materials for future fusion reactors, thanks to their higher swelling resistance, higher thermal conductivity, lower thermal expansion and better liquid–metal compatibility than austenitic steels [1]. For similar reasons, similar steels had been considered in the past for fast breeder reactors and are now being proposed for accelerator-driven systems and Gen-IV reactors. Their behaviour under irradiation has been extensively studied for the last 30 years. These studies have overall confirmed the suitability of high-Cr steels to withstand prolonged exposition to neutron irradiation. However, no experimental facility currently exists capable of reproducing the hard neutron

* Corresponding author. Tel.: +32 14 333090; fax: +32 14 321216.
E-mail address: lmalerba@sckcen.be (L. Malerba).

0022-3115/$ - see front matter © 2005 Elsevier B.V. All rights reserved.
doi:10.1016/j.jnucmat.2005.10.013

spectra at high doses of a fusion environment. Thus, the in-service behaviour of these steels must be in fact *extrapolated* to the real conditions. In order to do so in a correct way, it is important not only to test the material under ever more realistic conditions, but also to reach a reasonable level of understanding of the physical phenomena which drive the material response to irradiation as a function of dose and temperature. Moreover, it has been clearly observed that the composition of these steels, particularly the Cr content, determines a sometimes radically different behaviour during and after irradiation. For example, a minimum in ductile–brittle transition temperature increase due to irradiation is observed at about 9 wt% Cr [2]. In addition, neutron irradiation experiments on Fe–Cr alloys show that adding Cr up to a concentration of 12–15 wt% leads to a pronounced decrease in swelling compared to pure α-Fe, as well as to austenitic steels, with a non-monotonous and often fairly complicated dependence on Cr concentration, dose and irradiation temperature [3–7]. To date, no clear explanation exists for the mechanisms producing this dependence on Cr concentration of important macroscopic parameters defining the mechanical stability under neutron irradiation of these steels. The development of models to rationalise these observations is therefore an important part of nuclear reactor materials research.

The starting point for any neutron-irradiation damage modelling effort is the study of the primary state of damage produced by displacement cascades in the relevant material. Molecular dynamics (MD) is well known to be a suitable simulation tool for the study of displacement cascades and the analysis of the mechanisms of formation and motion of interstitial atoms and their clusters [8,9], provided that a valid and adequately stiffened many-body interatomic potential is available for the system of interest. In the past, much work has been done on MD simulation of displacement cascades, using pure Fe as model alloy for steels, described by a variety of interatomic potentials [10–14]. A critical review of the results of such work can be found in [15]. Additional work on displacement cascades in pure α-Fe is presented in [16], where the results obtained using four recent interatomic potentials are reported. To take a step forward toward modelling real engineering materials, the assessment of the effect of Cr – the main alloying element in RAFM steels – on the primary damage state is of critical importance. The work reported here provides a set of results on displacement cascades initiated by Fe recoils up to 50 keV in Fe–10at.%Cr. The simulations have been performed using a recently fitted and validated many-body potential for the Fe–Cr system [17,18]. Simulations done with this potential in pure Fe show that the results obtained with it for cascades are acceptable and consistent with existing results, within the relevant uncertainty [15,16]. The objective of the reported work is to study, analyse and discuss the main effects of the presence of Cr in terms of primary defect population, with special focus on the study of in-cascade interstitial cluster formation in Fe and Fe–10at.%Cr alloys. This work extends and completes preliminary results partly anticipated in [19,20].

2. Simulation method

2.1. Interatomic potential

The details of the fitting procedure and validation of the Embedded Atom Method (EAM) [21] interatomic potential for Fe–Cr used in this work can be found elsewhere [17,18]. Herein only the highlights will be summarised.

The Fe–Fe part was fabricated following the approach described in [22], using bulk modulus (1731 kbar), elastic constants ($C' = 525$ kbar, $C_{44} = 1219$ kbar), lattice parameter (0.2866 nm), cohesive energy (4.28 eV) and unrelaxed vacancy formation energy (1.60 eV) as fitting parameters, and stiffened using the same method as in [10]. It is noteworthy that this Fe–Fe potential provides an excellent reproduction of the experimentally measured phonon dispersion curves, as shown in Fig. 1 [23]. In addition, it predicts a melting point of about 1815 K, extremely close to the real one [25]. Its main shortcoming is that, like most long-range interatomic potentials for α-Fe [15], it provides reversed stability for the self-interstitial atom, i.e. the ⟨1 1 1⟩ crowdion is predicted as more stable than the ⟨1 1 0⟩ dumbbell, contrary to experimental evidence [26]. Nonetheless, it has been clearly shown that the results for displacement cascades obtained with this potential are in line with published results provided by other potentials for α-Fe, including potentials that feature the correct interstitial configuration stability, as well as with the results obtained using more recent potentials, and that no clear correlation exists between the predicted interstitial configuration stability and the outcome of cascade simulations with a given potential [15,16].

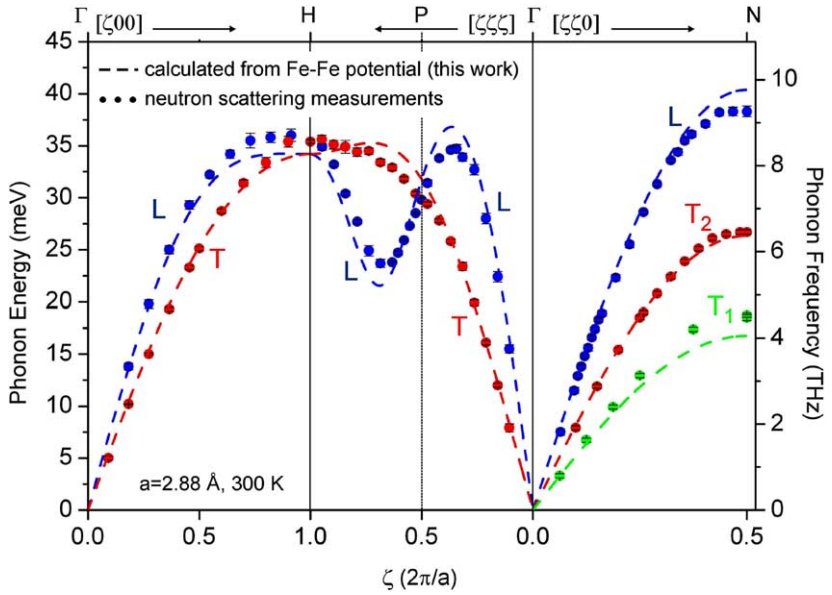

Fig. 1. Phonon dispersion curves as calculated using the potential for α-Fe which provides the Fe–Fe contribution to the Fe–Cr potential used in this work. Experimental points are from [24,25].

The Cr–Cr potential was taken from literature [27].

The Fe–Cr crossed pair contribution was fitted, using the procedure described in [28], to the experimental values of bulk modulus (1571 kbar), cohesive energy (−4.262 eV) and lattice parameter (0.2866 nm) for the Fe–10at.%Cr alloy, as well as to the mixing enthalpy of the same alloy (5.16 meV), obtained by ab initio methods allowing for the effect of ferromagnetism [29].

This Fe–Cr potential has proven to provide a reasonably good description of the interaction between Cr atoms and point defects in a ferritic matrix, when compared to density functional theory (DFT) results obtained with the VASP code [30], as illustrated in Table 1. The ab initio calculations reported in this table were done in the generalised gradient approximation (GGA) [31] with polarised spin. Results from two different methods are compared, namely fully non-local Vanderbilt-type ultra-soft pseudo-potentials (USPP) [32], with a cut-off energy of 240 eV, and projector augmented wave (PAW) pseudo-potentials [33,34], with cut-off energy of 350 eV. Data are given for both 54 and 128 atom supercells, dimensioned with the equilibrium lattice parameter for Fe (0.28544 nm with USPP, 0.282299 nm with PAW). The k point sampling was $5\times5\times5$ and $3\times3\times3$ with, respectively, 54 and 128 atom supercells. Ionic relaxations were always conducted, at constant volume, applying periodic boundary conditions. For details about the convergence and validation of results obtained in this way, see Ref. [35]. The

Table 1
Binding energies between Cr atoms and elementary point-defects in an Fe matrix: comparison between DFT data and empirical interatomic potential results

Defect	Binding energies (eV)				
	Potential	USPP-54	USPP-128	PAW-54	PAW-128
Cr–V (1 nn)	**0.035**	0.029	0.010	0.078	0.082
Fe–Cr ⟨1 1 0⟩	*0.27*	0.00	0.05	0.11	0.12
Fe–Cr ⟨1 1 1⟩	**0.33**	0.36	0.37	0.41	0.42
Cr–Cr ⟨1 1 0⟩	*0.48*	−0.55	−0.44	−0.33	−0.30
Cr–Cr ⟨1 1 1⟩	**0.46**	0.04	0.06	0.33	0.34

V is a vacancy. 'Fe–Cr' indicates a mixed dumbbell, 'Cr–Cr' indicates a dumbbell containing two Cr atoms; the direction of the dumbbell is specified. Note, however, that in the case of the Fe–Cr ⟨1 1 1⟩ defect, the stable configuration is actually, in all cases, a Cr-centred crowdion.

complete set of ab initio data concerning Fe–Cr is reported in full detail in [36].

The binding energies given in Table 1 are defined as differences between the total energy of the system containing the defect when the Cr atom(s) is(are) far away from it and when the Cr atom(s) is(are) close to, or inside, the defect. Thus, positive values indicate attraction and favoured configurations. This table shows that, although even DFT results are numerically different depending on the method applied (it is generally agreed that PAW should, in case of uncertainties, be considered as more reliable), all calculations, including those performed with the empirical potential, do succeed in grasping the fundamental features of the interaction between Cr atoms and point defects, namely, negligible interaction with the vacancy and significant interaction with the interstitial. These are suggested also by a series of results that can be found in the scientific literature.

Early resistivity recovery studies in Fe–Cr alloys of different compositions [37–39] were interpreted in terms of either strongly bound mixed Fe–Cr dumbbells, or the effect of the repulsion between Fe–Fe dumbbells and Cr atoms. In the 'strong binding' interpretation, Fe–Cr dumbbells were assumed to have a migration energy slightly lower than Fe–Fe dumbbells, but to be likely to be trapped by a second Cr atom [37]. This interpretation postulates the existence of an attractive, valency- and/or magnetic-driven interaction between Cr atoms and SIA's. In the 'repulsion interpretation', the explanation was based on the simple fact that Cr is slightly oversized compared to Fe [38,39]. Although the overall effect of the two interpretations is the same, i.e. suppression of SIA migration, the 'repulsion' one was later confuted, and the 'strong binding' one supported, by further, more thorough resistivity recovery studies, which clearly proved the existence of attractive interaction between SIA and solute atoms in Fe–Cr alloys [40–42]. Experiments also show that the addition of even small percentages (0.1 at.%) of Cr to ultra-pure Fe induces more frequent nucleation of small interstitial loops than in ultra-pure Fe [43], that the observed loop density is enhanced in electron-irradiated Fe–10 wt%Cr at 25 °C as compared to pure Fe [44] and that in α-Fe interstitial loop motion is significantly slowed down, and loop thermal stability significantly increased, by the presence of Cr [45]. All of these facts point to the existence of strong interaction between Cr and interstitial clusters.

Concerning the negligible interaction between Cr atoms and vacancies, Demangeat calculated, using a full-electron method, the V–Cr binding energy to be in any case below 0.089 eV [46] and muon spin rotation measurements by Möslang et al. showed later that the V–Cr binding energy in Fe is in any case less than 0.1 eV (i.e. below the resolution of the technique) [47]. In addition, according to positron annihilation experiments coupled to resistivity recovery studies, it has been observed that the onset of vacancy migration in pure Fe and Fe–Cr occurs at the same temperature, thereby concluding that Cr negligibly affects the mobility of vacancies in Fe alloys [38–40,48], except for a possible slight reduction of the migration energy [40]. It is also known that the solute diffusion of Cr in Fe (D_{Cr}) is extremely close to, although higher than, the self-diffusion of Fe (D_{Fe}) in a large range of Cr concentrations [49,50]: a sign of negligible V–Cr binding energy. It has been shown that the present potential predicts satisfactorily well the experimental D_{Cr}/D_{Fe} ratio [25,51].

Thus, although the present empirical potential somewhat overestimates the binding energy for the $\langle 1\,1\,0\rangle$ mixed dumbbell and gets the wrong sign for the binding energy of the $\langle 1\,1\,0\rangle$ Cr–Cr dumbbell, it can overall be considered satisfactory, at least to assess, as first approximation, the effect of this strong interaction with interstitials in the simulation of displacement cascades.

Note that the wrongly positive binding energy provided by the empirical potential in the case of the $\langle 1\,1\,0\rangle$ Cr–Cr dumbbell stems from a broader problem, related to the difficulty of reproducing the complicated thermodynamics of Fe–Cr alloys. It is known that below 9–10% Cr (at ~700 K) there is complete miscibility of Cr in Fe, with a tendency towards ordering (negative short-range order – SRO – parameter) [52], which can be promoted by both thermal ageing and irradiation [53–55]. On the other hand, within a miscibility gap starting above 9–10% Cr, the Cr-rich (more than 80% Cr) α′ phase is known to separate when the alloy is aged at intermediate temperatures (400–550 °C) [56–58], a phenomenon historically known as '475 °C embrittlement' [59]. In high-Cr ferritic/martensitic steels under irradiation, the uniform precipitation of α′-phase, together with other features (carbides, χ-phases, σ-phase, ...), has been also connected to embrittlement [60,61]. In Fe–Cr alloys this phase separation occurs following a nucleation and growth process for low enough Cr concentrations,

but corresponds to a spinodal decomposition starting at about 20% Cr [62–64]. In addition, in a restricted range of temperature and compositions, around 50% Cr and 500 °C, the σ-phase becomes stable [65]. From the atomic point of view all this means that two Cr atoms in otherwise pure Fe 'prefer' to be as far from each other as possible and that the binding energy between two nearest neighbour Cr atoms in Fe should be negative, thereby partly explaining the unfavourable $\langle 1\,1\,0\rangle$ Cr–Cr dumbbell in ab initio calculations, unless the local solute concentration becomes high enough to screen the repulsion, leading to a favourable aggregation of Cr atoms in the α' phase. From the thermodynamic point of view, the same phenomenon corresponds to a negative mixing enthalpy for low Cr concentrations, which becomes positive for high enough solute content. All this is indeed correctly predicted by DFT calculations [29,36], but not by the empirical potential, which was fitted to a positive mixing enthalpy and therefore provides a positive excess energy for all Cr concentrations. Caro et al. have indeed pointed out that, in order to closely reproduce the thermodynamic functions of binary alloys, the classical EAM is insufficient and some new, concentration-dependent potential formalism is required [66]. Progress is being made toward the fabrication of concentration-dependent, thermodynamically more correct potentials for Fe–Cr [67], which will be used for future simulation work. The present potential cannot be used in the range of compositions where either ordering or α' phase segregation are expected and for this reason, although it is believed that cascade-induced phase transformation is unlikely, displacement cascades where only simulated at the composition to which the potential was fitted, i.e. 10 at.% Cr. This concentration is safe because around it the thermodynamic forces leading to phase changes are, also in reality, vanishing.

To conclude about the potential used in this work, it has been calculated using the method illustrated in [68] that the threshold displacement energies of a single Cr atom in an Fe–10at.%Cr alloy is essentially the same as for an Fe atom in the same alloy (see Table 2). Although no direct experimental determination of threshold displacement energies in Fe–Cr alloys has been performed to the authors' knowledge, resistivity damage recovery curves could indeed be fitted to the same threshold displacement energy for Fe and Fe–10at.%Cr [38].

2.2. Cascade simulation

The above-described potential was implemented in the classical MD code Dymoka, which is suitable for the simulation of displacement cascades [14]. Prior to initiating the cascade, a block was equilibrated for 1 ps at 300 K. This initial atom block was then used as starting point for cascade simulation and reference for defect detection. The cascade was initiated by imparting a kinetic energy E_{MD} to the selected primary knock-on atom (PKA) along a high-index direction such as $\langle 135\rangle$ [10,13]. The cubic box size, simulated time and number of cascades versus E_{MD} are summarised in Table 3. No electronic stopping or electron–phonon coupling was included in the simulations. Following common practice [8–11,13,14], no attempt was made to control the temperature of the system and all results were obtained in the NVE microcanonical ensemble, with periodic boundary conditions. It is indeed accepted that the final simulation temperature rise scarcely influences the defect population generated in displacement cascades in Fe [13,69]. This temperature rise, which varies as a function of E_{MD} and the produced defect distribution, was at any rate in no case seen to exceed 200 K.

The evolution of the cascades was followed by studying selected representative snapshots.

Table 2
Threshold displacement energies of Fe and Cr atoms (in eV) according to the present potential in Fe, Cr and Fe–10%Cr, obtained using the method illustrated in [68]

Case	Threshold displacement energies (eV)				
	$\langle 1\,0\,0\rangle$	$\langle 1\,1\,0\rangle$	$\langle 1\,1\,1\rangle$	Mean	Median
Fe–Fe	20	48	30	54.5 ± 0.5	54
Cr–Cr	16	34	28	44.2 ± 0.4	44
Fe–Fe10%Cr	22	54	30	53.4 ± 0.5	52
Cr–Fe10%Cr	18	40	30	54.4 ± 0.6	54

Values are given for the three principal crystallographic directions. Mean and median value over all directions are also indicated.

Table 3
Summary of cascade simulation number and features in this work

Energy (keV)	Simulation time (ps)	No. (successful) cascades	Box side (a_0)	Atoms in the box (10^3)
0.5	10	20	30	54
0.7	10	20	30	54
1	10	10	30	54
2	10	10	40	128
5	20	10	50	128
8	20	10	50	250
10	30	10	50	432
15	30	10	65	~550
20	30	7	65	~550
30	30	7	73	~780
40	30	7	73	~780
50	30	5	73	~780

Intermediate and final atomic configurations were analysed to detect and count defects, using a Wigner–Seitz cell method: an empty cell corresponds to a vacancy, while two atoms in the same cell correspond to an interstitial configuration. Since, from the standpoint of the analysis, interstitial configurations are always identified as two atoms sharing the same cell, in what follows the term *dumbbell* will generally be used instead of *crowdion*, to stress the fact that the two atoms involved may or not be of the same chemical species (Fe–Fe, Fe–Cr, Cr–Cr). However, according to the potential used, interstitial configurations are always $\langle 1\,1\,1\rangle$ crowdions, which can be divided in two families, depending on the nature of the interstitial atom located at the centre of the crowdion configuration: Fe-centred and Cr-centred crowdions. The defect distribution and evolution were monitored using appropriate visualisation tools.

The cascade volume and density were assessed using the component analysis method [70,71]. With this method, the volume of the cascade is associated to an ellipsoid, whose axes are defined based on the variance of the spatial point-defect distribution. The major axis has the direction maximising the variance, the second one maximises the variance of the distribution projected onto a plane perpendicular to the first one, and the third one has the direction minimising this variance. These directions are parallel to the directions of the eigenvectors of the covariance matrix of the point-defect distributions and the associated eigenvalues are the variances of the distribution projected onto the directions of the eigenvectors. Thus, the problem is reduced to the diagonalisation of a 3×3 symmetrical, real and positive matrix, which is a straightforward operation. This method to define the cascade volume is clearly not completely justified when subcascade formation becomes important, i.e. above 20 keV. It provides nevertheless a reference for purely comparison purposes if used systematically for all cascades.

Particular attention was devoted to study the influence of Cr on the formation and main features of clusters. These were defined using a third nearest neighbour (nn) criterion for interstitials and second nn criterion for vacancies and have been detected using an automated procedure. The use of this procedure for interstitials has been seen to underestimate by about 16% the fraction evaluated through visual inspection [20]. However, the trend remains unaffected, so that its use allows a consistent (and faster) comparison between different cases. The discussion of the previous sections makes it unlikely that Cr can influence vacancy clustering, but effects on the interstitial population should be visible.

Interstitial clusters can be formed in cascades according to at least three mechanisms. They may be formed when a high-density part, produced during the ballistic phase and lingered on into the nearly melted zone created by the thermal spike, is isolated by a re-crystallisation front [72]. Partly they may also form at the end of the thermal spike, as a consequence of collective atomic motion in conditions of enhanced defect diffusion, due to high local temperature [9]. Finally, further interstitial clusters formation and growth may occur by later local defect re-organisation, driven by strain-field interaction among neighbouring interstitials and small clusters [9]. While the presence of interstitial-trapping solute atoms can hardly affect the first of these mechanisms, the other two are expected to be greatly influenced by it and the questions addressed here is how and up to what extent this influence can manifest itself.

3. Results

3.1. Peak time features

Peak time is defined as the time elapsed between the cascade initiation and the moment when the largest number of atomic defects is produced, independently of the fact that later most of them will be reabsorbed during the subsequent thermal spike and recombination phase (relaxation). This interval of time grows as a function of cascade energy, as

shown in Fig. 2 for cascades in both pure Fe and Fe–10%Cr. The figure shows that the growth of peak time is slowed down above 20 keV, a behaviour that can be ascribed to cascade splitting: parallel, almost concomitant sub-cascades, induced by secondary knock-on atoms of lower energy than the PKA, reach their peak almost simultaneously and reduce the overall peak time, on average, to a value closer to that of lower energy single cascades. The origin of the smaller step between 1–2 and 5 keV is, on the other hand, unclear, but should perhaps be connected to the onset of full cascade regime, as discussed in Ref. [10]. At any rate, the presence of Cr does not affect in any discernible way the peak time associated with the cascades of different energies.

The number of defects at peak time is shown in Fig. 3 versus cascade energy for both Fe and Fe–Cr. Except for a change of slope at low energy, it increases linearly with energy, as is broadly expected to do, if the NRT model assumption [73] is accepted for the ballistic phase. The presence of Cr does not appear to affect the results in any systematic way.

The average cascade volume, evaluated as explained in Section 2.2, is plotted versus cascade energy in Fig. 4. Note that the slightly faster increase of the volume above 20 keV is likely to be ascribable to cascade splitting, which causes also part of the 'undamaged' inter-sub-cascade volume to be included in the component analysis, used in this case at the verge of its limit of physical validity. However, in the present framework this shortcoming is irrelevant because the only objective is to determine whether the presence of Cr has or not an effect on the cascade volume and it appears that is has no influence. It can therefore be concluded that no Cr effect can be detected on the ballistic phase of the cascade in an Fe–Cr alloy, as compared to pure Fe.

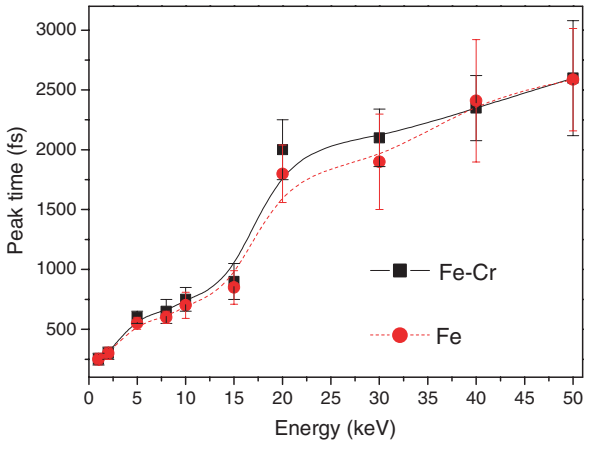

Fig. 2. Peak time versus energy for cascades in Fe and Fe–10%Cr. The lines correspond to polynomial splines.

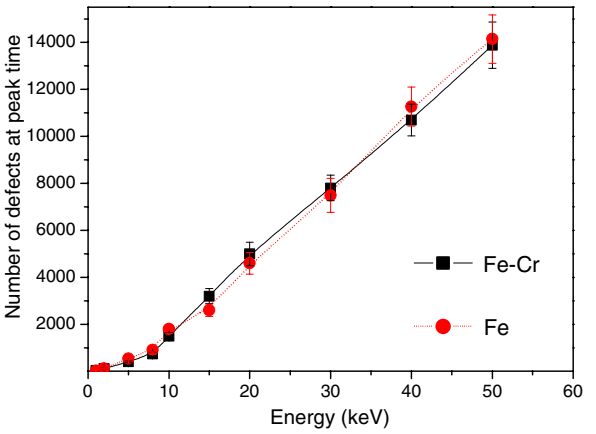

Fig. 3. Number of defects at peak time versus cascade energy in Fe and Fe–10%Cr.

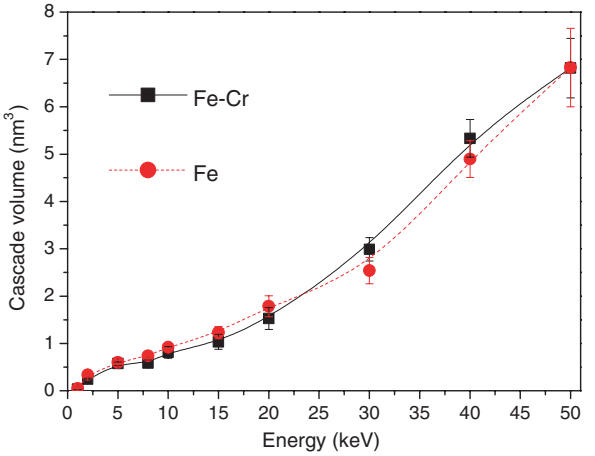

Fig. 4. Cascade volume versus energy in Fe and Fe–10%Cr.

3.2. Surviving defects

3.2.1. Frenkel pairs and dumbbells

At the end of the cascade, after relaxation, only a reduced fraction of the Frenkel pairs produced at peak time survives the thermal-spike-enhanced recombination process. The increase of their number as a function of the cascade energy, denoted as ν_{FP}^{end}, is illustrated in Fig. 5 for both pure Fe and Fe–10at.%Cr. The points have been interpolated using the empirical power law proposed by

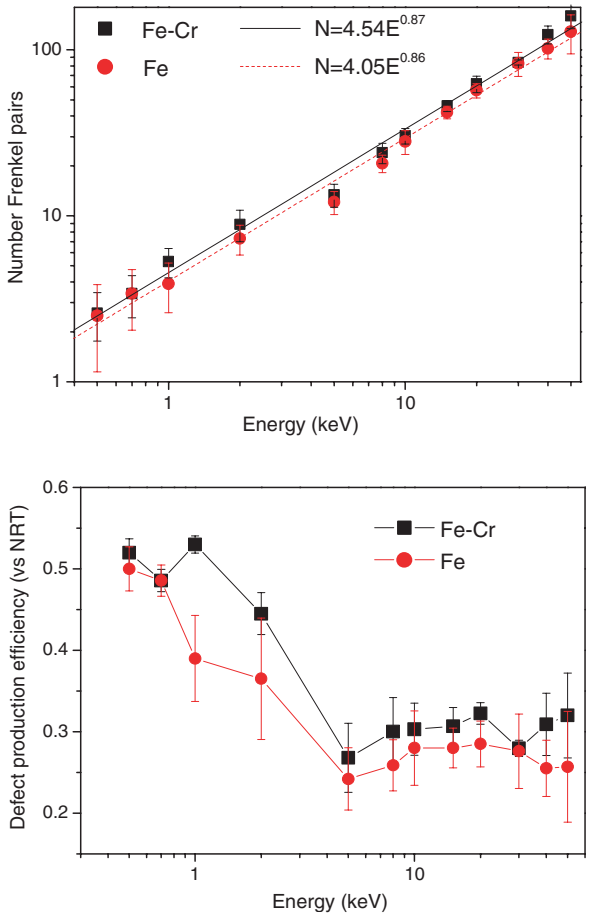

Fig. 5. Number of surviving Frenkel pairs (above) and their ratio to the NRT [73] value (below) versus cascade energy in Fe and Fe–10%Cr.

Bacon et al., $\nu_{FP}^{end} = A \cdot E_{MD}^{m}$ [8]. This formula is used here only for convenience and has therefore been extended to cover the whole range of data up to 50 keV, in spite of the fact that its validity with a constant exponent has been determined to be limited to the range from about 1 to 20 keV [13]. By splitting the data into two groups, above and below this threshold, slightly lower exponents (0.82) can be obtained for the low energy range, while exponents close to unity characterise the points at higher energy, in agreement with the discussion reported in [13], based on the idea of cascade splitting above 20 keV.

The defect production efficiency is also plotted in Fig. 5. This is defined as $\eta = \nu_{FP}^{end}/\nu_{NRT}$, where $\nu_{NRT} = 0.8E_D/2E_d$ [73]. In the latter formula, E_d is the average displacement energy for all crystallographic directions and E_D is the damage energy, i.e. E_D is the fraction of recoil energy that goes into displacive damage, after subtracting the portion dissipated for electron excitation. Since the interaction between ions and electrons is not included in the present MD simulations, it is assumed that $E_D = E_{MD}$. In addition, for the sake of simplicity and following Refs. [74,38], we took $E_d = 40$ eV for both pure Fe and Fe–10at.%Cr. Both these assumptions are customary in the case of pure Fe [8,9,13] and according to our estimate of threshold displacement energies of Cr atoms in Fe–10%Cr (Table 2) there is no reason to change the value of E_d because of the presence of Cr. The defect production efficiency decreases with recoil energy down to a more or less asymptotic value of about 0.3 (0.26 in Fe and 0.32 in Fe–Cr), in agreement with previous work on Fe [8,13,14] and within the range suggested by semi-experimental assessments of this magnitude for pure Fe [75–80]. The inspection of both graphs in Fig. 5 reveals a slightly higher defect production when Cr is present, which appears to be systematic and statistically significant. Possible reasons for this small difference are addressed in Section 4.

Although it may seem that Cr hardly affects the primary state of damage in Fe alloys, in fact it does have an important effect. By looking at the chemical nature of the produced dumbbells, it is found out that the number of mixed (Fe–Cr) dumbbells is remarkably higher than the number of Fe–Fe dumbbells at the end of lower energy cascades, and equal at higher energies, as is shown in Fig. 6. The same figure shows that the fraction of Fe–Cr dumbbells is higher than, or around, 50% of the total, to be compared with the 10% Cr concentration in the alloy.

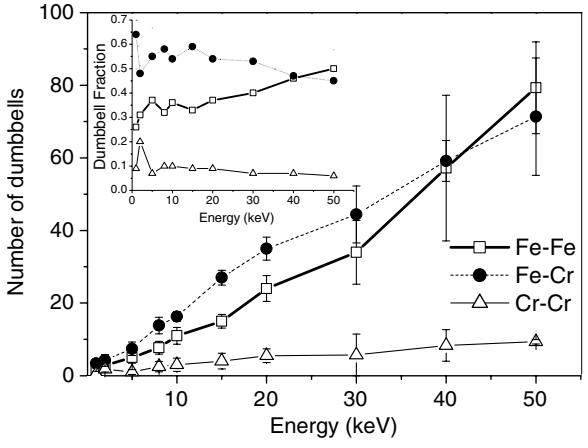

Fig. 6. Number and fraction (inset) of dumbbells versus cascade energy in Fe–10%Cr.

Clearly, the favoured formation of mixed dumbbells is a consequence of the binding energy between interstitials and Cr atoms predicted by this potential. A discussion about the process whereby this high fraction of mixed dumbbells is produced and why it appears to decrease with cascade energy is provided in Section 4, together with a suggestion of the possible consequences of this fact on the long-term evolution of the system. Here it is important to emphasise that, although the prediction of the present interatomic potential cannot be considered fully quantitative, the discussion in Section 2.1 suggests that it is at least qualitatively acceptable and in agreement with a number of experimental facts. For example, evidence of Cr enrichment at the edge of large loops in Fe–Cr alloys has been reported by Yoshida et al. [44]. Thus, the present effect of *more-than-stoichiometric* presence of Cr in interstitial defects is likely to be real, and not just an artefact of the potential. Quantitative differences expected when using potentials featuring better descriptions of interstitial configurations in α-Fe are discussed in Section 4.

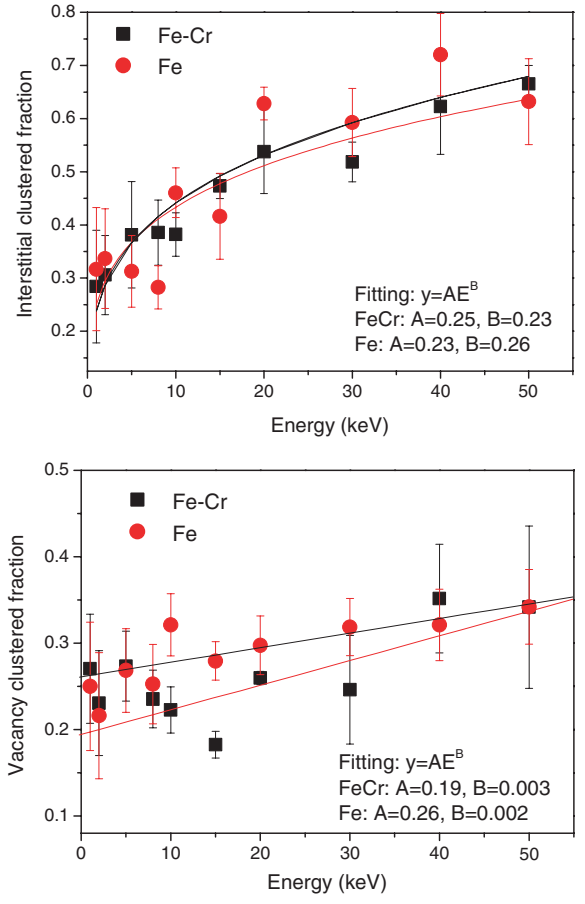

Fig. 7. Clustered fraction of interstitials (above) and vacancies (below) versus recoil energy for cascades in Fe and Fe–10%Cr.

3.2.2. Clusters

Fig. 7 displays the fraction of defects in clusters at the end of the cascade (last snapshot) for both interstitials and vacancies in Fe and Fe–10%Cr as a function of cascade energy. It can be said that the presence of Cr does not influence either the amount of interstitials, or the amount of vacancies

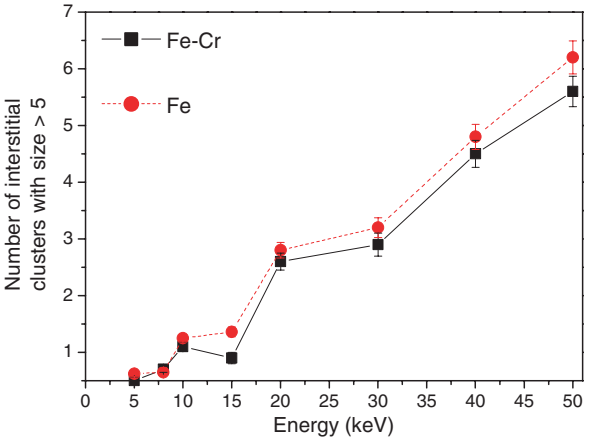

Fig. 8. Number of interstitial clusters of size larger than five as a function of cascade energy in Fe and Fe–10%Cr.

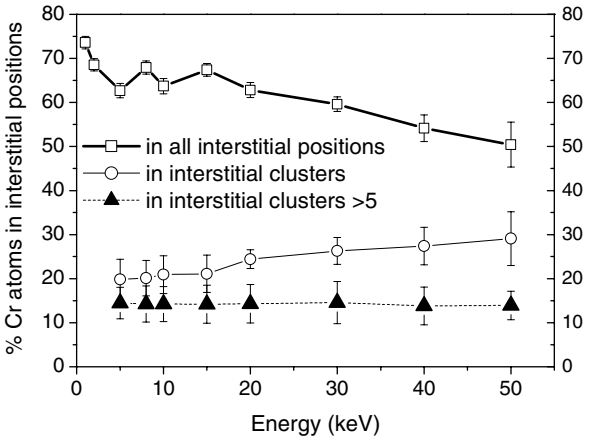

Fig. 9. Fraction of Cr atoms in interstitial position versus cascade energy. Squares denote the ratio of Cr atoms in dumbbells to the total number of atoms involved in interstitial configurations (thus, Cr–Cr dumbbells count for two Cr atoms). Circles denote the fraction of Cr atoms inside interstitial clusters only and triangles focus on the fraction in clusters of size larger than five.

that end up in clusters. The size distribution is only marginally affected: in Fig. 8 the average number of interstitial clusters of size larger than five is seen to be systematically smaller in Fe–10%Cr compared to pure Fe, but the difference is small.

Concerning the chemical composition of clusters, Fig. 9 reveals that most interstitial Cr atoms belong to isolated dumbbells. Nonetheless, also the concentration of Cr in interstitial clusters remains higher than the concentration of the alloy, although it gets closer and closer to the latter with increasing cluster size. The possible mechanisms leading to the accumulation of Cr atoms in interstitial position, both in clusters and outside, are discussed in the next section.

4. Discussion

The study of the threshold displacement energies in a ferritic matrix, summarised in Table 2, shows that only in one of the three main crystallographic directions, namely ⟨1 1 0⟩, the threshold for Cr atoms is somewhat lower than for Fe atoms in Fe–10%Cr. The mean and median values are essentially coincident. In addition, Fig. 3 demonstrates that, at the peak of the ballistic phase, the number of displacements in Fe and Fe–10%Cr is essentially the same. Finally, the discussion in Ref. [16] suggests that, generally, the value of the threshold energy has little or no influence on the outcome of the cascade. Thus, the slightly higher number of surviving defects in the alloy cannot be explained with a different threshold energy for Cr atoms. It must therefore be the effect of the observed formation of stable Fe–Cr and Cr–Cr dumbbells during cascade cooling, which trap and stabilise interstitials and therefore reduce, slightly, the probability of defect annihilation.

The formation of a number of mixed dumbbells higher than, or comparable to, the number of Fe–Fe dumbbells at the end of the cascade is a phenomenon that takes place during the relaxation phase, at least according to the present potential. This is illustrated in Fig. 10, where the number of dumbbells of different types is plotted versus time in the case of a 10 and a 20 keV cascade. During the ballistic phase more Fe atoms than Cr atoms are displaced and counted as interstitials, roughly in a proportion similar to the alloy composition. However, during the cooling stage most of these Fe-crowdions, possibly assisted by the still high temperature, glide until they get trapped at the closest Cr atoms, thereby determining a cross-over of the curves at ~4.5 and ~20 ps for 10 and 20 keV, respectively.

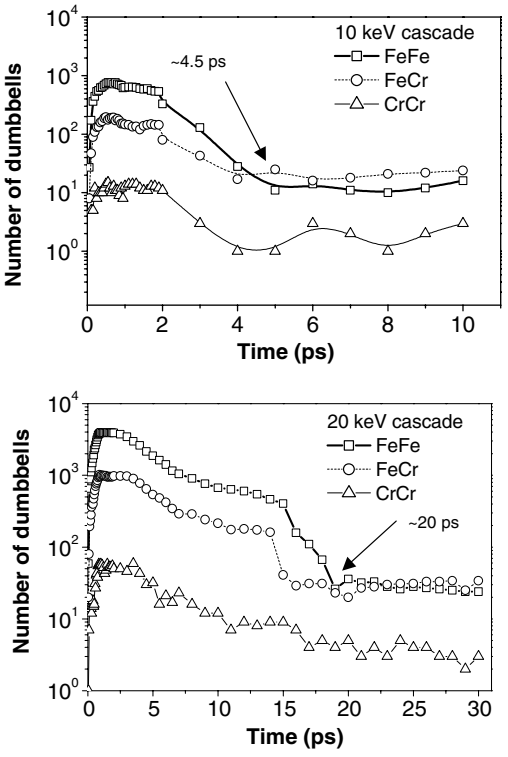

Fig. 10. Number of dumbbells of different type as a function of time in a 10 keV (above) and a 20 keV (below) cascade: the Cr enrichment of the interstitial population is a post-collisional phenomenon.

The fraction of Fe–Cr dumbbells, although always much larger than the Cr concentration in the alloy, decreases with increasing cascade energy (Fig. 6). This is probably due to the fact that the fraction of interstitials in clusters increases with energy (Fig. 7) and that the concentration of Cr in isolated interstitials is significantly higher than in interstitial clusters (Fig. 9). This fact is again to be ascribed to the high stability of the Cr-crowdion and the absence of a mechanism (at least with this potential) whereby the Cr interstitial can move and remain, at the same time, at the centre of a crowdion. Indeed, supposing that the trapping barrier is overcome and that the Cr-crowdion glides along its ⟨1 1 1⟩ direction (the only migration mechanism predicted by this potential), the interstitial atom becomes an Fe atom. In other words, Cr-crowdions, once formed after the thermal spike, essentially do not move and therefore cannot join clusters during the local interstitial re-organisation

driven by elastic interaction. Nor will they glide towards possible available vacancies, thereby slightly increasing the number of surviving defects. Only Fe interstitials can efficiently gather and form clusters. Thus, more interstitials in clusters means globally less 'free' single interstitials suitable for being 'captured' by Cr atoms and, therefore, less Cr atoms in interstitial position.

Nonetheless, the percentage of Cr atoms in interstitial clusters is also higher than the average alloy concentration. As mentioned in Section 2.2, interstitial clusters are formed in cascades in Fe partly at an early stage as a consequence of re-crystallisation, partly at the end of the thermal spike, as a consequence of collective atomic motion, and partly later, via local defect re-organisation, driven by elastic interactions among interstitial defects. Two possible explanations can therefore be put forward for the large concentration of Cr atoms in clusters [20]. One is that Cr atoms gathered collectively in the interstitial clusters either during the ballistic phase or, more likely, at the end of the thermal spike, when high temperature enhances defect diffusion and mixing, the cooling process eventually favouring the final interstitial location of Cr atoms. The other is that, during local re-organisation, interstitial cluster formation is favoured in regions with a pre-existing higher local Cr concentration. In other words, in regions of higher local Cr concentrations interstitials may be more likely to remain trapped because of the presence of Cr atoms (which become interstitial atoms), thereby acting as nuclei for further cluster growth. Or, equivalently, pre-formed small clusters containing only Fe-crowdions may migrate and get trapped in regions of higher local Cr concentration, where they can also further grow. Fig. 11 suggests that the latter mechanism is the most likely one: the Cr concentration in interstitial clusters increases after the thermal spike has come to an end, the growth being more pronounced for higher energies, when larger interstitial clusters are formed (Figs. 7 and 8). This behaviour must be interpreted as the result of a post-relaxation re-distribution of interstitials and interstitial clusters in regions of locally higher Cr concentration.

Thus, it appears that the main difference between the primary damage state in pure Fe and Fe–Cr alloys is the presence of a large population of Fe–Cr dumbbells and the fact that Cr atoms are preferentially associated to interstitial clusters as well.

What remains to be discussed is up to what extent the results obtained with the present potential can be

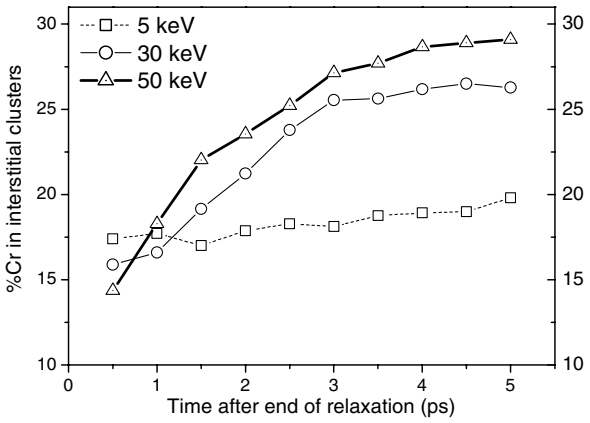

Fig. 11. Evolution in time of the fraction of Cr atoms in interstitial clusters after the end of the relaxation phase (after which the number of defects remains roughly stable) for three cascades of different energy.

generalised, considering that the configuration, and therefore the migration mechanism, of the single interstitial is not correctly described. More precisely, according to the present potential single interstitials can only glide along ⟨1 1 1⟩ directions, with negligible probability of change of direction at room temperature (one-dimensional diffusion) and with a very low migration energy (around 0.06 eV) [51]. In contrast, single interstitials in Fe (and therefore in Fe–Cr) are known, on the basis of both experimental [26] and ab initio [81] studies, to migrate three-dimensionally, maintaining a ⟨1 1 0⟩ dumbbell configuration, with a migration energy of about 0.3 eV. This fact seems to invalidate the present study, at least as far as the final, diffusional stage of the cascade is concerned. However, three facts need to be remembered. Firstly, only very recently a potential for α-Fe capable of predicting the correct interstitial migration energy, in agreement with ab initio calculations, has been proposed [82,83]: most cascade results available from literature and used as reference were in any case obtained with potentials featuring not completely correct descriptions of interstitials; yet, the results can be considered broadly acceptable, as recently reviewed [15]. Secondly, the existence of a non-negligible binding energy between interstitials and Cr atoms must be considered as a proven fact (see Section 2.1), and this feature is allowed for by the present potential. Thirdly, interstitial clusters in α-Fe above a certain size are one-dimensionally migrating collections of ⟨1 1 1⟩ crowdions, as demonstrated by a variety of classical molecular dynamics studies [12,13,84,85], using different potentials, and ab initio [83] calculations, and this feature too is

fairly well described by the present potential. Thus, we can state that, while the quantitative significance of the results obtained with this potential for the association of Cr atoms to single interstitials may be partly questioned, the results concerning the association of Cr atoms to clusters can be largely considered valid.

For slowly migrating single ⟨1 1 0⟩ dumbbells, such as those expected to be found in real α-Fe and more or less correctly predicted by a number of existing potentials, the processes leading to their getting trapped at Cr atoms might be less effective, or slower, than the present potential predicts for single interstitials. In particular, no fast glide toward the closest Cr atoms will occur. So, the amount of isolated mixed dumbbells produced in cascades may be less spectacular than the present potential shows. Nonetheless, provided that a binding energy exists, it will still be significant, because three-dimensionally migrating interstitials have any way, in the long term, more chances of finding a trap than one-dimensionally migrating ones and, in addition, differently from solute-centred crowdions, mixed dumbbells can migrate as such, i.e. once the mixed dumbbell is formed it will not be 'broken' by the process of interstitial migration. This possibility of mixed dumbbell migration will not only enhance the effective stability of mixed dumbbells, but also favour the formation of clusters containing a significant amount of Cr atoms by aggregation of single interstitials, a process forbidden in the case of crowdions, as pointed out above. At the same time, also with more realistic potentials clusters formed in cascades will still be of ⟨1 1 1⟩ type, and will still glide one-dimensionally toward regions of high Cr concentration, where they will get trapped. Thus, provided that a binding energy with Cr atoms of the order predicted by ab initio calculations (Table 1) exists, a final concentration of Cr atoms in interstitial position larger than the alloy concentration will also be observed using potentials featuring a more correct description of interstitial configurations and lower single-interstitial mobility. Only quantitative differences may be found, probably in the sense that less mixed dumbbells and, perhaps, a higher amount of Cr in interstitial clusters may be detected. However, only further work with now available advanced potentials [67] can support these speculations.

The key information provided by the present potential which, we believe, will remain true independently of the potential used and represents a useful piece of information to be retained in order to model the evolution of the system beyond the primary state of damage is the following: Cr atoms are traps for interstitial clusters but the number, size and nature of the interstitial clusters produced in cascades in Fe–Cr alloys will essentially be the same as in pure Fe. In addition, trapping will be more effective in the case of smaller clusters, which appear to contain a higher fraction of Cr atoms. It must indeed be emphasised that the association of Cr atoms to interstitial clusters is likely to be more important to determine the long-term evolution of the microstructure under irradiation than the formation of mixed dumbbells which, in any case, are experimentally known to exist and to migrate with an energy very close to the energy of Fe–Fe dumbbells [37,40,42]. Of course, the existence of mixed dumbbells may lead to anomalous diffusion and therefore have an influence on segregation phenomena. However, it has been calculated that the trapping of interstitial clusters at Cr atoms produces a drastic reduction of their mobility in the alloy compared to pure Fe [86]. This effect agrees with recent experimental observations [45] and provides a key for the interpretation of many of the experimental results mentioned in the introductory part of this work, such as the accumulation of a larger density of smaller clusters in Fe–Cr alloys under electron irradiation [43,44]. In particular, the swelling behaviour of Fe–Cr alloys versus Cr concentration [3–7] can be explained in terms of the suppression of interstitial cluster motion, possibly modulated by phase changes induced by irradiation at high enough doses. The investigation of these issues is the focus of ongoing work [86].

5. Summary and conclusions

Displacement cascades in Fe and Fe–10%Cr alloys have been simulated by molecular dynamics in a range of energies from less than 1 keV up to 50 keV. The interatomic potential used, in spite of its inherent limitations, which have been extensively discussed, provides cascade results for pure Fe which are consistent with previous work and has been proven to describe correctly, both qualitatively and quantitatively, the interaction between Cr atoms and point defects in ferritic alloys, when compared to experimental and first principle indications. It has been observed that

- the presence of Cr does not affect the ballistic phase of the cascade, in terms of number of atomic displacements, volume and density. The

final population of defects and clusters is only slightly altered: a few more Frenkel pairs survive recombination and clusters are slightly smaller in Fe–10%Cr than in pure Fe;

- these effects are connected to the high affinity of Cr atoms for interstitial positions, which manifests itself in a large population of Fe–Cr dumbbells, in proportion well above the Cr concentration in the alloy, as well as in a preferential association of Cr atoms to interstitial clusters;
- the build-up of the large Cr concentration in interstitial defects is a process that takes place in the post-collisional and post-relaxation phases, through short-range migration and re-distribution of interstitials: single interstitials migrate till they remain trapped at Cr atoms, while clusters tend to form or to grow and coalesce in regions of higher local Cr concentration, where their mobility is reduced;
- there are reasons to believe that these features, although with possible quantitative differences, or through somewhat different mechanisms, will remain true independently of the potential used in the simulations, provided that the potential used predicts binding energies between interstitials and Cr atoms in agreement with existing ab initio calculations;
- it is particularly important to know, for longer timescale modelling, that interstitial clusters produced in cascades are trapped by Cr atoms and that the number, size and type of clusters is for the rest extremely similar to pure Fe.

The trapping of interstitials and, more importantly, interstitial clusters due to Cr atoms in Fe alloys not only broadly agrees with experimental indications, but in fact provides a valuable key for the interpretation of the yet unexplained behaviour of Fe–Cr alloys versus solute content, particularly concerning reduced swelling and enhanced nucleation of interstitial loops compared to pure Fe.

Acknowledgements

The authors are grateful to C. Domain (EDF) for providing ab initio calculation results and assistance with the Dymoka code, as well as for fruitful discussions. This work, partially supported by the European Commission under the contract of Association between EURATOM and the Belgian State, was carried out within the framework of the European Fusion Development Agreement (EFDA), task TTMS-007.

References

[1] R.L. Klueh, K. Ehrlich, F. Abe, J. Nucl. Mater. 191–194 (1992) 116.
[2] A. Kohyama, A. Hishinuma, D.S. Gelles, R.L. Klueh, K. Ehrlich, J. Nucl. Mater. 233–237 (1996) 138.
[3] E.A. Little, D.A. Stow, J. Nucl. Mater. 87 (1979) 25.
[4] D.S. Gelles, J. Nucl. Mater. 108&109 (1982) 515.
[5] S.I. Porollo, A.M. Dvoriashin, A.N. Vorobyev, Yu.V. Konobeev, J. Nucl. Mater. (1998) 247.
[6] F.A. Garner, M.B. Toloczko, B.H. Sencer, J. Nucl. Mater. 276 (2000) 123.
[7] B.H. Sencer, F.A. Garner, J. Nucl. Mater. 283–287 (2000) 164.
[8] D.J. Bacon, A.F. Calder, F. Gao, V.G. Kapinos, S.J. Wooding, Nucl. Instrum. and Meth. B 102 (1995) 37.
[9] D.J. Bacon, A.F. Calder, F. Gao, J. Nucl. Mater. 251 (1997) 1.
[10] A.F. Calder, D.J. Bacon, J. Nucl. Mater. 207 (1993) 25.
[11] R. Vascon, N.V. Doan, Rad. Eff. Def. Solids 141 (1997) 375.
[12] N. Soneda, T. Díaz de la Rubia, Phil. Mag. A 78 (1998) 995.
[13] R.E. Stoller, J. Nucl. Mater. 276 (2000) 22;
R.E. Stoller, G.R. Odette, B.D. Wirth, J. Nucl. Mater. 251 (1997) 49.
[14] C.S. Becquart, C. Domain, A. Legris, J.-C. van Duysen, J. Nucl. Mater. 280 (2000) 73.
[15] L. Malerba, J. Nucl. Mater., in press.
[16] D. Terentyev, C. Lagerstedt, P. Olsson, K. Nordlund, J. Wallenius, C.S. Becquart, L. Malerba, J. Nucl. Mater., in press.
[17] R. Chakarova, V. Pontikis, J. Wallenius, Development of Fe(bcc)–Cr many body potential and cohesion model, WP6 Delivery Report Nr. 6, SPIRE project, EC contract no. FIKW-CT-2000-00058, June 2002. Available from: <www.neutron.kth.se/publications/library/DR-6.pdf>.
[18] P. Olsson, L. Malerba, A. Almazouzi, A first step towards a multiscale modelling of Fe–Cr alloys, SCKCEN Report, BLG-950, June 2003.
[19] L. Malerba, D.A. Terentyev, P. Olsson, R. Chakarova, J. Wallenius, J. Nucl. Mater. 329–333 (2004) 1156.
[20] D.A. Terentyev, L. Malerba, M. Hou, Nucl. Instrum. and Meth. B 228 (2005) 156.
[21] M.S. Daw, M.I. Baskes, Phys. Rev. B 29 (1984) 6440.
[22] G. Simonelli, R. Pasianot, E.J. Savino, Mater. Res. Soc. Symp. Proc. 291 (1993) 567.
[23] M. Rieth, unpublished work.
[24] V.J. Minkiewicz, J. Shirane, R. Nathans, Phys. Rev. 162 (1967) 528.
[25] D.A. Terentyev, L. Malerba, P. Olsson, M. Hou, in: A.I. Melker (Ed.), Seventh International Workshop on Nondestructive Testing and Computer Simulations in Science and Engineering (NDTCS-7, St. Petersburg, Russia, 9–15 June 2003), Proceedings of the International Society of Optical Engineering, vol. 5400, SPIE, Bellingham, WA, 2004, ISBN 0-8194-5323-4, p. 85 (ISSN: 0277-786X).
[26] P. Ehrhart, K.H. Robrock, H.R. Schober, in: R.A. Johnson, A.N. Orlov (Eds.), Physics of Radiation Effects in Crystals, Elsevier, Amsterdam, 1986, p. 7, and references therein.

[27] D. Farkas, C.G. Schon, M.S.F. de Lima, H. Goldstein, Acta Mater. 44 (1996) 409.
[28] A.F. Voter, in: J.H. Westbrook, R.L. Fleischer (Eds.), Intermetallic Compounds: Vol. 1, Principles, Wiley, New York, 1995.
[29] P. Olsson, I.A. Abrikosov, L. Vitos, J. Wallenius, J. Nucl. Mater. 321 (2003) 84.
[30] G. Kresse, J. Hafner, Phys. Rev. B 47 (1993) 558; G. Kresse, J. Hafner, Phys. Rev. B 49 (1993) 14251.
[31] J.P. Perdew, Y. Wang, Phys. Rev. B 45 (1992) 13244.
[32] D. Vanderbilt, Phys. Rev. B 41 (1990) 7892; G. Kresse, J. Hafner, J. Phys.: Condens. Matter. 6 (1996) 8245.
[33] P.E. Blöchl, Phys. Rev. B 50 (1994) 17953.
[34] G. Kresse, D. Joubert, Phys. Rev. B 59 (1999) 1758.
[35] C. Domain, C.S. Becquart, Phys. Rev. B 65 (2001) 024103.
[36] P. Olsson, PhD dissertation, Acta Universitatis Uppsaliensis (2005), ISSN 1651-6214, ISBN 91-554-6365-7.
[37] F. Maury, P. Lucasson, A. Lucasson, F. Faodo, J. Bigot, J. Phys.: Metal. Phys. 17 (1987) 1143.
[38] A. Benkaddour, C. Dimitrov, O. Dimitrov, Mater. Sci. Forum 15–18 (1987) 1263.
[39] C. Dimitrov, A. Benkaddour, C. Corbel, P. Moser, Ann. Chim. Fr. 16 (1991) 319.
[40] A.L. Nikolaev, V.L. Arbuzov, A.E. Davletshin, J. Phys.: Condens. Matter. 9 (1997) 4385.
[41] H. Abe, E. Kuramoto, J. Nucl. Mater. 271&272 (1999) 209.
[42] A.L. Nikolaev, J. Phys.: Condens. Matter. 11 (1999) 8633.
[43] A. Okada, H. Maeda, K. Hamada, I. Ishida, J. Nucl. Mater. 256 (1999) 247.
[44] N. Yoshida, A. Yamaguchi, T. Muroga, Y. Miyamoto, K. Kitajima, J. Nucl. Mater. 155–157 (1988) 1232.
[45] K. Arakawa, M. Hatanaka, H. Mori, K. Ono, J. Nucl. Mater. 329–333 (2004) 1194.
[46] C. Demangeat, Phil. Mag. 32 (1975) 323.
[47] A. Möslang, E. Albert, E. Recknagel, A. Weidinger, Hyperf. Interact. 15&16 (1983) 409.
[48] E. Kuramoto, S. Nagano, K. Nishi, K. Makii, Y. Aono, M. Takenaka, Mater. Sci. Forum 105–110 (1992) 1125.
[49] A. Wolfe, H.W. Paxton, Trans. Met. Soc. AIME 230 (1964) 1426.
[50] A.M. Huntz, P. Guiraldenq, M. Aucoutourier, P. Lacombe, Mem. Sci. Rev. Metall. 66 (1969) 85.
[51] D. Terentyev, L. Malerba, J. Nucl. Mater. 329–333 (2004) 1161.
[52] I. Mirebeau, M. Hennion, G. Parette, Phys. Rev. Lett. 53 (1984) 687.
[53] H. Kuwano, Y. Hamaguchi, J. Nucl. Mater. 155–157 (1988) 1071.
[54] N.P. Filippova, V.A. Shabashov, A.L. Nikolaev, Phys. Met. Met. 90 (2000) 145.
[55] V.V. Sagaradze, I.I. Kositsyna, V.L. Arbuzov, V.A. Shabashov, Yu.I. Filippov, Phys. Met. Met. 92 (2001) 508.
[56] R.M. Fisher, E.J. Dulis, K.G. Carroll, Trans. AIME 197 (1953) 690.
[57] R. Lagneborg, Trans. ASM 60 (1967) 67.
[58] P.J. Grobner, Metall. Trans. 4 (1963) 251.
[59] H.D. Newell, Metals Progr. 49 (1949) 977.
[60] P. Dubuisson, D. Gilbon, J.L. Séran, J. Nucl. Mater. 205 (1993) 178.
[61] M.H. Mathon, Y. de Carlan, G. Geoffroy, X. Averty, A. Alamo, C.H. de Novion, J. Nucl. Mater. 312 (2003) 236.
[62] S.S. Brenner, M.K. Miller, W.A. Soffa, Scripta Metall. 16 (1982) 831.
[63] J.M. Hyde, M.K. Miller, A. Cerezo, G.D.W. Smith, Appl. Surf. Sci. 87&88 (1995) 311.
[64] F. Danoix, P. Auger, Mater. Charact. 44 (2000) 177.
[65] O. Kubaschewski, T.G. Chart, J. Inst. Met. 93 (1964–1965) 329.
[66] A. Caro, P.E.A. Turchi, M. Caro, E. Lopasso, J. Nucl. Mater. 336 (2005) 233.
[67] P. Olsson, J. Wallenius, C. Domain, K. Nordlund, L. Malerba, Phys. Rev. B, in press.
[68] K. Nordlund, J. Wallenius, L. Malerba, Nucl. Instrum. and Meth. B, in press.
[69] F. Gao, D.J. Bacon, P.E.J. Flewitt, T.A. Lewis, J. Nucl. Mater. 249 (1997) 77.
[70] M. Hou, Phys. Rev. B 31 (7) (1985) 4178.
[71] A. Souidi, M. Hou, C.S. Becquart, C. Domain, J. Nucl. Mater. 295 (2001) 179.
[72] K. Nordlund, M. Ghaly, R.S. Averback, M.-J. Caturla, T. Diaz de la Rubia, J. Tarus, Phys. Rev. B 57 (1998) 7556.
[73] M.J. Norgett, M.T. Robinson, I.M. Torrens, Nucl. Eng. Design 33 (1975) 50.
[74] Annual Book of ASTM Standard E693-94, vol. 12.02, 1994.
[75] M.A. Kirk, L.R. Greenwood, J. Nucl. Mater. 80 (1979) 159.
[76] P. Jung, Phys. Rev. B 23 (1981) 664.
[77] C. Jaouen, J.P. Rivière, C. Templier, J. Delafond, J. Nucl. Mater. 131 (1985) 11.
[78] S. Takamura, T. Aruga, K. Nakata, J. Nucl. Mater. 136 (1985) 159.
[79] G. Wallner, M.S. Anand, L.R. Greenwood, M.A. Kirk, W. Mansel, W. Waschkowski, J. Nucl. Mater. 152 (1988) 146.
[80] C.H.M. Broeders, A.Yu. Konobeyev, J. Nucl. Mater. 328 (2004) 197.
[81] C. Fu, F. Willaime, P. Ordejón, Phys. Rev. Lett. 92 (17) (2004) 175503.
[82] M.I. Mendelev, S. Han, D.J. Srolovitz, G.J. Ackland, D.Y. Sun, M. Asta, Phil. Mag. 83 (35) (2003) 3977.
[83] F. Willaime, C. Fu, M.C. Marinica, J. Dalla Torre, Nucl. Instrum. and Meth. B 228 (2005) 92.
[84] Yu.N. Osetsky, D.J. Bacon, A. Serra, B.N. Singh, S.I. Golubov, J. Nucl. Mater. 276 (2000) 65; Yu.N. Osetsky, A. Serra, B.N. Singh, S.I. Golubov, Phil. Mag. A 80 (9) (2000) 2131.
[85] Yu.N. Osetsky, D.J. Bacon, A. Serra, B.N. Singh, S.I. Golubov, Phil. Mag. 83 (1) (2003) 61.
[86] D.A. Terentyev, L. Malerba, A.V. Barashev, Phil. Mag. Lett., in press.